Life Sciences 268 (2021) 119009

Contents lists available at ScienceDirect

Life Sciences

journal homepage: www.elsevier.com/locate/lifescie

Long non-coding RNA and mRNA profile analysis in the parotid gland of mouse with type 2 diabetes

Yan Huang [a], Hui-Min Liu [b], Li-Ling Wu [b], Guang-Yan Yu [a,*], Ruo-Lan Xiang [b,**]

[a] Department of Oral and Maxillofacial Surgery, Peking University School and Hospital of Stomatology, National Engineering Laboratory for Digital and Material Technology of Stomatology and Beijing Key Laboratory of Digital Stomatology, Beijing 100081, PR China
[b] Department of Physiology and Pathophysiology, Peking University School of Basic Medical Sciences, Key Laboratory of Molecular Cardiovascular Sciences, Ministry of Education, and Beijing Key Laboratory of Cardiovascular Receptors Research, Beijing 100191, PR China

ARTICLE INFO

Keywords:
Diabetes mellitus
Parotid gland
Saliva secretion
Long non-coding RNA
Microarray analysis

ABSTRACT

Aims: Salivary gland dysfunction is a common complication of diabetes mellitus (DM). Long non-coding RNA (lncRNA) is evidenced to involve in the functional regulation of salivary gland, however, its role in DM-impaired gland is unknown. Therefore, this study aimed to investigate the expression profiles and functional networks of lncRNA in the parotid glands (PGs) of DM mice.

Main methods: Microarray was used to detect lncRNA and messenger RNA (mRNA) expression profiles in the PGs from db/db and db/m mice. Eleven differently expressed (DE) lncRNAs validated by qRT-PCR were selected for coding-non-coding gene co-expression (CNC) and competing endogenous RNA (ceRNA) network analysis, as well as the following Gene Ontology (GO) and Kyoto Encyclopedia of Genes and Genomes (KEGG) analysis. Pearson's coefficient correlation analysis was used to analyze the correlations between DE lncRNAs expression and DM pathology.

Key findings: By using a 2-fold change and $P < 0.05$ as the cutoff criteria, 1650 DE lncRNAs (758 upregulated and 892 downregulated) and 1073 mRNAs (563 upregulated and 510 downregulated) were identified in the PGs of db/db mice compared to db/m mice. GO and KEGG analysis of DE mRNA suggested that activated inflammation response and downregulated ion transport might count for the dysfunction of diabetic PG. CNC and ceRNA networks analysis of 11 DE lncRNAs showed that the inflammation process and its related signaling pathways including advanced glycation end product (AGE)-receptor for AGE (RAGE) signaling pathway in diabetic complications, cytokine-cytokine receptor interaction, chemokine signaling pathway, apoptosis, and cell adhesion molecules were significantly enriched. The alterations of lncRNAs were closely correlated with higher blood glucose and serum insulin levels in mice.

Significance: We identified multiple lncRNAs/mRNAs and several signaling pathways that may involve in the pathogenesis of diabetic salivary injury, providing new insight into potential target of diabetic hyposalivation.

1. Introduction

Diabetes mellitus (DM) is a group of metabolic disorders caused by insulin production deficiency or insulin resistance [1]. Abnormal glucose metabolism-induced hyperglycemia impairs the function of salivary gland, thereby reducing saliva secretion [2]. With the global epidemic of DM, an increasing number of people are suffering from a series of problems caused by hyposalivation, including speaking, chewing, tasting, and digesting difficulties [3]. Hence, it is worthwhile to investigate the underlying mechanism of diabetic hyposalivation.

Parotid gland (PG) is one of the three major salivary glands, contributing to 25% and 53% of total saliva in resting and stimulated state, respectively [4]. Clinical observations already find benign enlargement of PGs in patients with DM, accompanied by decreased salivary flow rates [5,6]. Further studies find that the structures of PGs in DM patients and rats are damaged, manifested as an accumulation of secreted granules and lipid droplets. All these indicate that both structure and function of PG are impaired under diabetic condition [7–11]. However, the underlying mechanism is largely unclear.

Long non-coding RNA (lncRNA) is a cluster of non-protein-coding

* Correspondence to: G-Y. Yu, Department of Oral and Maxillofacial Surgery, Peking University School and Hospital of Stomatology, Beijing 100081, PR China.
** Correspondence to: R-L. Xiang, Department of Physiology and Pathophysiology, Peking University School of Basic Medical Sciences, Beijing 100191, PR China.
E-mail addresses: gyyu@263.net (G.-Y. Yu), xiangrl@bjmu.edu.cn (R.-L. Xiang).

https://doi.org/10.1016/j.lfs.2020.119009
Received 13 November 2020; Received in revised form 24 December 2020; Accepted 28 December 2020
Available online 4 January 2021
0024-3205/

RNA with more than 200 nucleotides in length, which can function as signals, decoys, guides, and scaffolds in epigenetic, transcriptional, or post-transcriptional regulations [12,13]. Recently, an increasing number of lncRNA is emerging to play roles in salivary gland diseases. In labial salivary glands of primary Sjögren's syndrome (pSS) patients, lncRNA expression profile is changed, which may contribute to the pathophysiology of salivary glands by increasing autoimmune response [14–16]. Pleomorphic adenoma is a common tumor of salivary gland. Studies show that lncRNAs are differentially expressed (DE) in pleomorphic adenoma tissues from pleomorphic adenoma gene 1 transgenic mice as compared with those from control mice [17]. Moreover, lncRNA is reported to regulate insulin biosynthesis and secretion, as well as glucose and lipid metabolism, thereby participating in the pathophysiology of DM and its complications [18,19]. LncRNA CRNDE expression is negatively correlated with the expression of cardiac fibrosis marker genes. Overexpression of CRNDE attenuates cardiac fibrosis and enhances cardiac function in mice with diabetic cardiomyopathy [20]. Therefore, the expression profile and the potential role of lncRNA in the dysfunction of diabetic PG need to be identified.

The present study was designed to establish lncRNA and messenger RNA (mRNA) expression profiles in PGs from type 2 DM mice by microarray technology. Coding-non-coding gene co-expression (CNC) and competing endogenous RNA (ceRNA) networks, followed by Gene Ontology (GO) and Kyoto Encyclopedia of Genes and Genomes (KEGG) analysis of DE lncRNAs and mRNAs were constructed to investigate the potential functions of lncRNA, which may provide new directions for further mechanism studies on the dysfunction of diabetic PG.

2. Materials and methods

2.1. Animal experiments

Four 16-week-old male leptin receptor-deficient db/db mice weighing 40–55 g (a model of spontaneous type 2 DM) and age-matched db/m mice weighing 25–30 g were purchased from Changzhou Cavens Laboratory Animal Ltd. The animal experiment was approved by the Ethics Committee of Animal Research, Peking University Health Science Center (No. LA2019252) and complied with the ARRIVE guidelines as well as the National Institutes of Health Guide for the Care and Use of Laboratory Animals (NIH Publications No. 8023). Mice were housed in a humidity- and temperature-controlled room on a reversed 12 h light/dark cycle with free access to food and water. The animals were fasted for at least 6 h with water ad libitum before extraction. Blood glucose level was measured by a Glucometer (ACCU-CHEK). Serum insulin was detected by the Iodine [^{125}I]-Insulin Radioimmunoassay Kit (Union Medical & Pharmaceutical Technology Ltd.). Insulin resistance index (HOMA-IR) was calculated by the following formula: fasting insulin (mU/L) × fasting glucose (mmol/L)/22.5. After anesthesia with an intraperitoneal injection of chloral hydrate (0.4 g/kg body weight), the fresh PG samples were extracted and frozen with liquid nitrogen for 1–2 min, then stored at −80°C.

2.2. Microarray detection and analysis

Frozen PGs from db/m and db/db mice were cryo pulverized using biopulverizer (Biospec) and homogenized with TRIzol (Invitrogen Life Technologies) by Mini-Bead-Beater-16 (Biospec). RNA was collected from each sample based on the manufacturer's protocols. The quantity and integrity of purified RNA were evaluated using NanoDropND-1000 (Thermo Scientific) and Agilent 2100 bioanalyzer (Agilent Technologies). Microarray hybridization was performed using Agilent Gene Expression Hybridization Kit (Agilent Technologies) in hybridization chambers according to the manufacturer's instructions. The Agilent Feature Extraction Software (version 11.0.1.1) was used to analyze and extract array images. Quantile normalization and subsequent data processing were conducted in GeneSpring GX v12.1 software package (Agilent Technologies). Threshold defined as fold-change > 2.0 (Student's *t*-test, $P < 0.05$) was used as a volcano plot filtering for DE lncRNAs and mRNAs. The DE profiles of lncRNA and mRNA between db/m and db/db groups were presented by hierarchical clustering. All the microarray hybridization and analysis were carried out by KangChen Biotech (Shanghai, China). All the original data have been submitted to the GenBank databases with accession number GSE161162.

2.3. Reverse transcription PCR and quantitative real-time PCR

Total RNA was extracted from homogenized PG tissues using Trizol reagent (Invitrogen Life Technologies). For each sample, 2 μg RNA was reversed into cDNA using 5 × All-In-One RT MasterMix (Applied Biological Materials Inc.) according to the manufacturer's protocols. For quantitative real-time PCR (qRT-PCR), 10 μL reaction mixture including 5 μL of 2 × SYBR® Green Master Mix (Genstar), 2 μL of 1:3 diluted cDNA, and 1 μL of 10 nmol/L primer were incubated in a PikoReal Real-Time PCR System (Thermo Fisher Scientific) at 95°C for 5 min, and followed by 40 cycles of 95°C for 10 s and 60°C for 30 s. Data analysis was further conducted through PikoReal 2.0 software. The primer sequences of lncRNAs and mRNAs were displayed in Tables 1 and 2.

2.4. Gene Ontology and Kyoto Encyclopedia of Genes and Genomes enrichment analysis

The topGO (http://www.geneontology.org) was applied to conduct GO analysis of target genes on molecular function, biological process, and cellular component. KEGG pathway analysis (www.genome.jp/kegg) was applied to analyze the key regulatory pathways involved in the injury of diabetic PG. Furthermore, the enrichment score −log10 (*P* value) was calculated to analyze the significance of the differences in terms.

2.5. Coding-non-coding gene co-expression and competing endogenous RNA network analysis

The DE lncRNAs validated by qRT-PCR and related DE mRNAs were selected to construct CNC and ceRNA networks. The lncRNA-mRNA co-expression networks were constructed by calculating the Pearson correlation coefficients (PCC) and *P*-values between multiple genes using Cytoscape software (The Cytoscape Consortium). The transcripts were filtered using a PCC > 0.95 and $P < 0.05$. The targeted microRNAs (miRNAs) were predicted with miRNA target prediction software based on TargetScan and miRanda databases. LncRNA-miRNA-mRNA ceRNA networks were further constructed.

2.6. Statistical analysis

The numerical data were presented as mean ± standard error of the mean (SEM). Statistical analysis between two groups of normalized data was performed using the students' *t*-test in GraphPad Prism 5.0. Mann Whitney *U* test was used if the variances were significantly different through *F* test in SPSS 24. Correlation was conducted by Pearson's coefficient correlation analysis. A level of $P < 0.05$ was considered statistically significant.

3. Results

3.1. Differential expression of lncRNAs and mRNAs

A type 2 DM of db/db mice was validated by the higher blood glucose, serum insulin, and insulin resistance index compared to db/m mice (Fig. 1A–C). LncRNA and mRNA expression profiles of mice PGs were analyzed by microarray technology. The volcano plot analysis was used to assess variations in lncRNAs between two groups. Of the 33,802 lncRNAs in the microarray, 1650 lncRNAs were differentially expressed

Table 1
Primers for validated lncRNAs.

Gene	Forward primer (5′-3′)	Reverse primer (5′-3′)	Size (bp)
ENSMUST00000175668	CGGGAGTATTTGGAAATGAACCT	CTGGATAGCAGTGAAATGTCAGAAT	93
ENSMUST00000123574	CCGAGGCTACAAGGTGGAT	CTGTTGGTTACTGCCAAGCTATA	197
ENSMUST00000189909	TCCTGAGGCGAGCATTGGC	CTGTATTCCAAAAGTACCTGAAATC	81
ENSMUST00000146010	TTACGGATATTTCCTGAACGAC	CACATCGAAGCATTTATTCATAGT	176
uc008anr.1	CCTCTTCTGGAAATTCACAAA	TTCCTCTGAATAGTTGTTTCTTGA	199
ENSMUST00000147774	CTGATCAAGAACACCTGCCCT	GTCACCAACCTGAGACCACC	242
ENSMUST00000146884	TTCACTTCTCTTCCAGGTCTTT	AAGCAGGGTGCTCTTACAGT	292
ENSMUST00000099676	AGCAGGAGTCTAGCAGACAACC	TGGCAGAAGACTTTAACGACG	143
ENSMUST00000150947	CAGTACATTGGTGAACTGCTTC	GGCTACACATTTGCTCATCTTT	275
TCONS_00008179	GCTTGGGGCTGTCTTTATCC	TTGGGCTGTATGGAATGGG	171
uc.273-	AAATCTGCTCCAGGCTCACA	AGTGGTTTGTGGTGTTTTTGAG	70
TCONS_00002412	CGGCATACCGTCACTGTAAA	CCTCGGAAACCCAGCGAG	178
ENSMUST00000140392	TCCCATGTTTGGAGAGTGG	GATGAAGAAAATCCAGTAACCA	153
AK155805	CAGGCAGTTGGGTTGGTTT	CAGAATGGACTTACTCGGTGC	200
ENSMUST00000203799	GGAGTGCCGACACCAGAGT	CAGAAGCGTTGATGTAGCAGA	236
ENSMUST00000160089	TCGTGCCTGTTTCCCTGAAT	GGGCTGAGAGCTATGTGGAT	93
ENSMUST00000189055	TAAAGTCCTTCTTGATGTCCTCTAC	TTACTCTCTCGGGATCTCTCAG	189
ENSMUST00000128831	CTACGATGAGGACGTGTTGGC	CTGGAATGAAGGACCAATATCTCC	123
ENSMUST00000140814	TGGGACTTCCCTCCTCACA	ACGGCACTCGTACCAACC	100
ENSMUST00000210596	TTCAGTCACACAGCAACCCG	GGGTCACAGGACTTGGGATCT	173
β-actin	GTACCACCATGTACCCAGGC	AACGCAGCTCAGTAACAGTCC	247

Table 2
Primers for validated mRNAs.

Gene	Forward primer (5′-3′)	Reverse primer (5′-3′)	Size (bp)
Tnfrsf12a	CCTGGTCTGGAGAAGATGCC	TGAATGAATGGACGACGAGTG	138
Tspan3	GTGCTGGTCTTCCTCAACCT	CAGCTATGATCACCACGGCA	145
Hmgn3	CACCAACGTAGTCATTATGCC	AATCTTTGTTCCAGGTTCTTTC	184
Tmem176a	TGCCATCGTTATTGGGTCTC	TCCTCTGTTTCCGCCTTTGT	291
Hist1h4i	CATGTCTGGTCGTGGCAAAG	CCCTGGATGTTGTCCCGAA	87
Ms4a4b	TGTGAGAACACACAAGCAAAG	CTTTGAAGGCACAGCAACTCC	153
Cyr61	CGAGTTACCAATGACAACCCAG	TGCAGCACCGGCCATCTA	223
Chl1	CAGATCGGGGTGTGGATCAG	GAGGCAACGTGCAAAGACTG	300
Mmd	TGGACCCCTGGCATCTCATA	CATGGGCGAACGGAATGATG	254
Mastl	AATCTAGCTGGCGGGAGT	GGGCATCTCTCTCAGCTTGTA	295
Cyp2j13	CCTTTGTGGGCAACTCGTTC	CTGGCCACTGGAGAAGATCAA	245
Wfdc12	TTGGTCCTCATGACGCTCCT	CACCTTACTCTGAGGGATCTGT	237
Rprml	GCTCATCAAGTCCGAGAGCA	GTAGTCTCTTCCTCGCGGTG	139
Cyp4a31	TTGCCAGAATGGAGAATGAGG	CTTGGGACAGGTGGGTAGAGC	274
Nkx3–2	AACCGTCGCTACAAGACCAAAC	GACGCAGGAATCCTTCTTTGC	273
Scgb1b27	CAAGGCACAGGCAACCAGTC	GTGAGAGCAAGGATGTACCCAT	76
Tmc1	GTTGCCCTTTGACCTACTCCT	TGCTACGCTGAGAATACAGATACA	178
Scgb2b3	GCCTTCCTGGTGATTGGAGAG	TGATGCAACCAAAGCCTTTTCC	110
Slc27a5	GGACCACTGGACTCCCAAAG	GGTTGCTCAGGGACGTTACA	298
Slc27a2	CCTCCTGATGATCGACCGTG	AGGCACGCCATACACATTCA	154
β-actin	GTACCACCATGTACCCAGGC	AACGCAGCTCAGTAACAGTCC	247

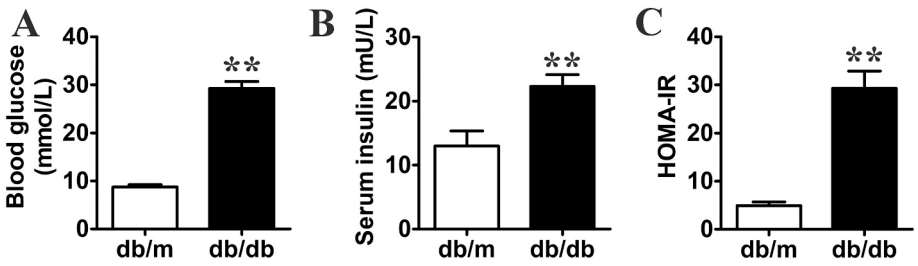

Fig. 1. Confirmation of db/db mice a type 2 diabetes mice model. (A) Blood glucose levels of db/m and db/db mice. (B) Serum insulin levels of db/m and db/db mice. (C) Insulin resistance index (HOMA-IR) of db/m and db/db mice. $^{**}P < 0.01$, versus db/m mice, n = 4.

in the PGs of db/db mice as compared to db/m mice (fold change > 2, $P < 0.05$). Among these lncRNAs, 758 were upregulated and 892 were downregulated (Fig. 2A). Hierarchical clustering map presented the top 30 upregulated and downregulated lncRNAs with raw intensity higher than 500 (Fig. 2B). The information of the top 10 upregulated and downregulated lncRNAs was shown in Table 3. Besides, a total of 1073 DE mRNAs were detected in db/db mice, including 563 upregulated and 510 downregulated, which were depicted in the volcano plot (Fig. 2C) and heat map (Fig. 2D). The 10 mRNAs with the largest fold changes in both upregulated and downregulated groups were displayed in Table 4.

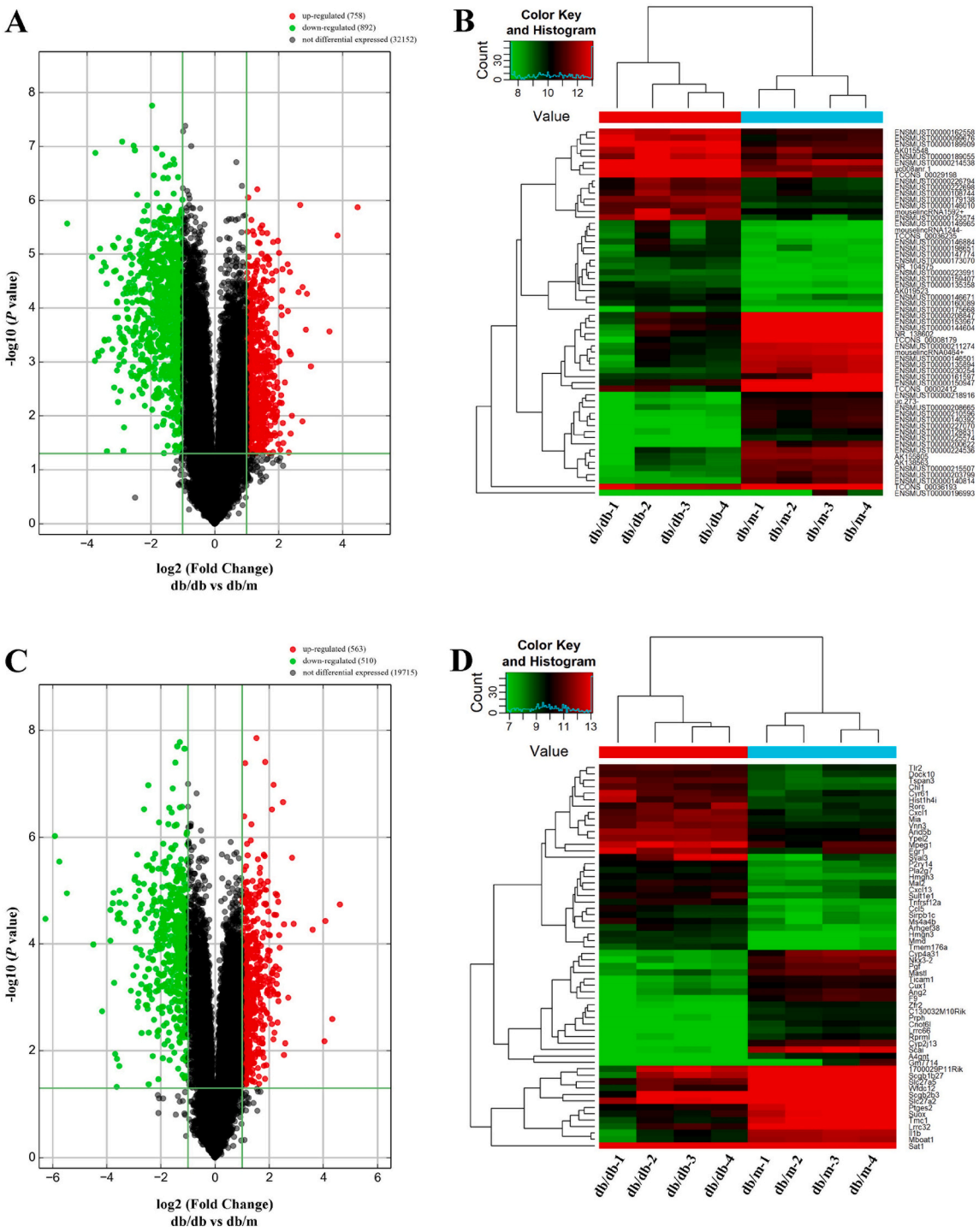

Fig. 2. Differentially expressed lncRNAs and mRNAs in PGs of db/db mice comparing to db/m mice. (A) Volcano plots presenting differences in the expression of lncRNAs between db/db mice and db/m mice. (B) Heat map of top 30 upregulated and downregulated lncRNAs with raw intensity higher than 500. (C) Volcano plots presenting differences in the expression of mRNAs between db/db mice and db/m mice. (D) Heat map of top 30 upregulated and downregulated mRNAs with raw intensity higher than 500. Values plotted on the x- and y-axes represent the averaged normalized signal values of each group (log2-scaled). LncRNA, long non-coding RNA; mRNA, massage RNA; PG, parotid gland.

3.2. Validation of differentially expressed lncRNAs and mRNAs

To confirm the results of microarray, the top 20 DE lncRNAs and mRNAs were assessed by qRT-PCR. Among 20 DE lncRNAs, 12 lncRNAs were consistent with the microarray data. The results of 8 lncRNAs including ENSMUST00000099676, ENSMUST00000123574, ENSMUST00000146010, ENSMUST00000147774, ENSMUST00000160089, ENSMUST00000175668, ENSMUST00000189055, and ENSMUST00000189909 were upregulated, while 4 lncRNAs including AK155805, ENSMUST00000140392, ENSMUST00000140814, and ENSMUST00000150947 were downregulated in the PGs of db/db mice (Fig. 3A, B). The results of mRNA expression showed that 14 mRNAs including 8 upregulated (Tnfrsf12a, Tspan3, Hmgn3, Tmem176a, Hist1h4i, Ms4a4b, Chl1, and Mmd) and 6 downregulated (Cyp2j13, Wfdc12,

Table 3
Top ten upregulated and downregulated lncRNAs of parotid glands in db/db mice.

Gene ID	Source	Chrome	Fold change	*P*-value	Regulation	Class
AK132892	Genbank	chrY	22.2417014	0.042319953	Up	Intergenic
ENSMUSG00000108415	GENCODE	chr7	14.3670564	0.011624392	Up	Intergenic
AK138488	Genbank	chr9	12.0713866	0.010513206	Up	Intergenic
AK051538	Genbank	chr3	8.0676053	0.000396168	Up	Intergenic
ENSMUSG00000086070	GENCODE	chr4	7.4184764	0.028916828	Up	Intergenic
uc.146	UCR	chr3	7.2478759	0.016735571	Up	Intergenic
ENSMUSG00000095913	GENCODE	chr19	6.7277821	0.001804149	Up	Antisense
AK045249	Genbank	chr13	5.3530787	0.017868446	Up	Intronic
ENSMUSG00000021519	GENCODE	chr13	5.2149984	0.000766994	Up	Sence
ENSMUSG00000114851	GENCODE	chr13	5.1150718	0.017279288	Up	Intergenic
ENSMUSG00000087112	GENCODE	chr19	24.556398	0.000433013	Down	Intergenic
ENSMUSG00000091021	GENCODE	chr4	14.2993657	0.015806423	Down	Antisense
humanlincRNA1009	lincRNA	chr12	13.4327799	7.46672E−05	Down	Sence
AK080127	Genbank	chr8	13.3184864	6.96531E−05	Down	Intergenic
ENSMUSG00000113741	GENCODE	chr12	12.6590183	7.20025E−05	Down	Antisense
ENSMUSG00000028060	GENCODE	chr3	12.4492871	2.71488E−06	Down	Sence
AK042825	Genbank	chr1	12.035163	0.004025192	Down	Intergenic
ENSMUSG00000087422	GENCODE	chr2	11.640126	7.79065E−05	Down	Intergenic
ENSMUSG00000031375	GENCODE	chrX	11.5410492	4.60976E−05	Down	Sence
ENSMUSG00000089934	GENCODE	chr10	11.5410492	0.000108254	Down	Intronic

Table 4
Top ten upregulated and downregulated mRNAs of parotid glands in db/db mice.

Gene symbol	Chrome	Fold change	*P*-value	Regulation
Gm29776	chr14	24.477149	0.00197521	Up
4921507P07Rik	chr6	20.1282934	0.038240957	Up
Wdr6	chr9	16.8519151	0.001257043	Up
Tmem9	chr1	16.4588434	0.000406055	Up
Tlr12	chr4	12.185125	0.000258672	Up
H2-Ab1	chr1	7.4956671	0.003861202	Up
Chst7	chrX	7.2018267	0.002970704	Up
Rbmxl2	chr7	6.5105383	0.018590881	Up
Mmp3	chr9	6.0435891	0.007259566	Up
Adamdec1	chr14	5.8511154	0.000305935	Up
Slc7a11	chr3	76.9199729	0.001765477	Down
Srrm4	chr5	60.4193821	0.000592696	Down
Cux1	chr5	53.8490878	0.001532157	Down
Tnxb	chr17	44.3879746	0.000340051	Down
Rprml	chr11	22.5600639	0.001822389	Down
Mkks	chr2	18.0295058	0.000192472	Down
Hmga2	chr10	14.587775	0.000786123	Down
Olfr883	chr9	14.5681586	0.007079982	Down
Plb1	chr5	13.719538	0.00022701	Down
ccdc198	chr14	13.3956077	0.000295879	Down

Rprml, Scgb2b3, Slc27a5, and Slc27a2) were in accordance to microarray data (Fig. 3C, D).

3.3. Gene Ontology and Kyoto Encyclopedia of Genes and Genomes analysis of differentially expressed mRNAs

We next performed GO analysis to determine the potential biological role of the DE mRNAs. The GO results indicated that the upregulated mRNAs were involved in 64 cellular components, 1289 biological processes, and 116 molecular functions. Among them, the most significantly enriched cellular component was cell periphery (Fig. 4A). For biological process, the top 5 GO terms were immune system process, regulation of immune system process, cell activation, positive regulation of response to stimulus, and leukocyte activation (Fig. 4B). In addition, the top 5 enriched molecular functions of upregulated mRNAs were binding, protein binding, chemokine activity, chemokine receptor binding, and fibronectin binding (Fig. 4C). Meanwhile, GO analysis of downregulated mRNAs showed involvements in 60 cellular components, 409 biological processes, and 90 molecular functions. According to enrichment score, the most significantly enriched cellular component was cell part (Fig. 4D). Xenobiotic metabolic process, ion transport, negative regulation of biological process, regulation of ion transport, and positive regulation of ion transport were significantly enriched biological processes of downregulated mRNAs (Fig. 4E). For molecular functions, ion transmembrane transporter activity, inorganic molecular entity transmembrane transporter activity, and transmembrane transporter activity were significantly enriched (Fig. 4F).

KEGG pathway analysis of DE mRNAs determined 86 altered pathways in the PGs of db/db mice including 68 upregulated and 18 downregulated. The upregulated mRNAs in the PGs of db/db mice were significantly involved in the pathways like cytokine-cytokine receptor interaction, osteoclast differentiation, chemokine signaling pathway, *Staphylococcus aureus* infection, and rheumatoid arthritis (Fig. 4G). The notable pathways including arachidonic acid metabolism, linoleic acid metabolism, serotonergic synapse, cortisol synthesis and secretion, and inflammatory mediator regulation of transient receptor potential channels were associated with the downregulated mRNAs (Fig. 4H).

3.4. Coding-non-coding gene co-expression network analysis

In order to identify co-expressed mRNAs of DE lncRNAs in diabetic PG, 11 lncRNAs (fold change > 2, $P < 0.05$), excepting for ENSMUST00000147774 which was validated to be upregulated less than 2 folds in the qRT-PCR experiment, were selected to conduct the lncRNA-mRNA interaction and co-expression network using Cytoscape v2.8.3.4. GO analysis on co-expressed mRNAs presented that these mRNAs were involved in 78 cellular components, 1266 biological processes, and 127 molecular functions. The significantly enriched GO terms were immune system process, cell activation, biological adhesion, cell adhesion, and leukocyte activation in biological processes and cell periphery, plasma membrane, cell part, cell, and extracellular region in cellular components (Fig. 5A, B). In addition, the molecular functions of binding, protein binding, protein dimerization activity, signaling pattern recognition receptor activity, and pattern recognition receptor activity were significantly enriched (Fig. 5C). KEGG pathway analysis showed that the co-expressed mRNAs were mostly enriched in advanced glycation end product (AGE)-receptor for AGE (RAGE) signaling pathway in diabetic complications, cytokine-cytokine receptor interaction, chemokine signaling pathway, malaria, and osteoclast differentiation (Fig. 5D).

We then chose the top 3 signaling pathways with higher enrichment scores in KEGG analysis and set the PCC of lncRNA and mRNA co-expression at above 0.95 to draw lncRNA-mRNA interaction and co-expression networks. As showed in the network, a total number of 34 DE mRNAs were related to 7 DE lncRNAs involving in AGE-RAGE

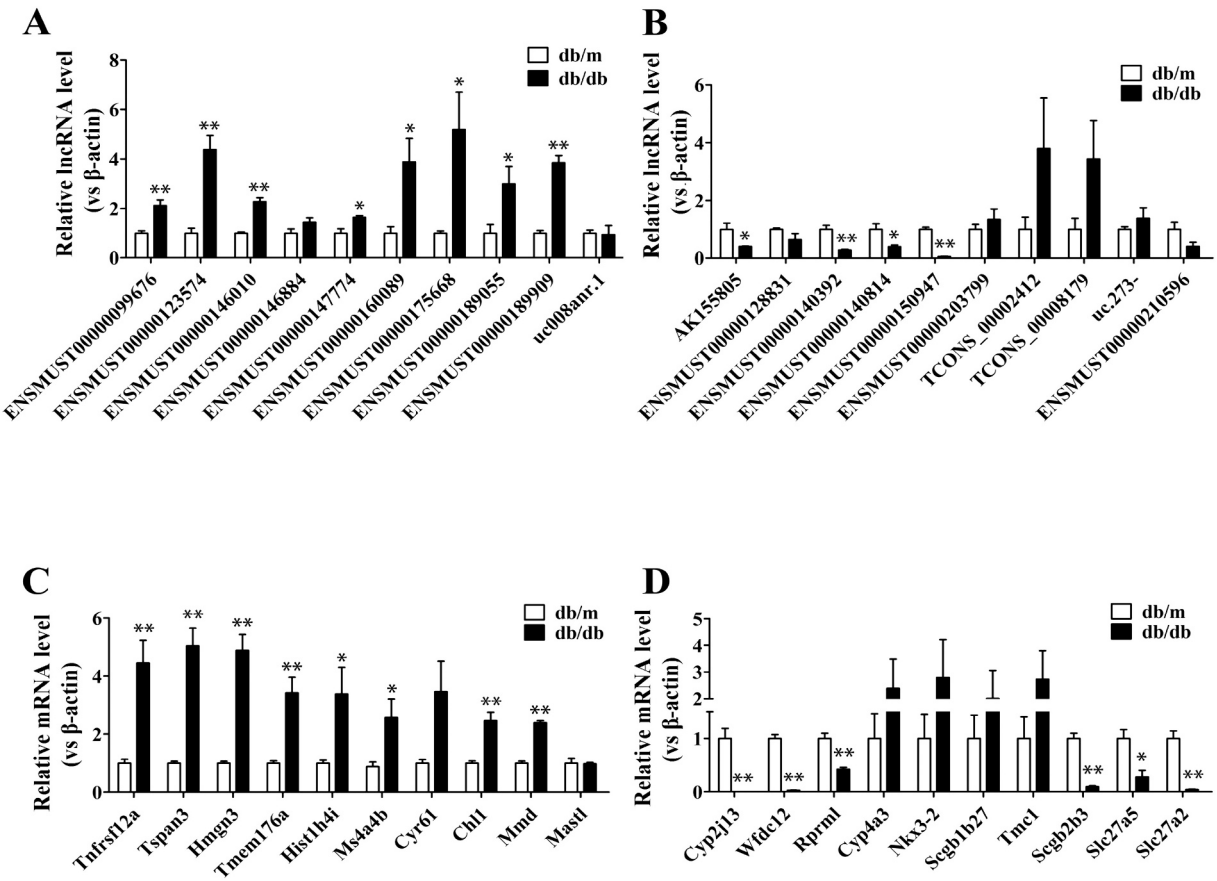

Fig. 3. Validation of differently expressed lncRNAs and mRNAs by qRT-PCR. (A) Expression of selected 10 upregulated lncRNAs in db/db mice and db/m mice. (B) Expression of selected 10 downregulated lncRNAs in db/db mice and db/m mice. (C) Expression of selected 10 upregulated mRNAs in db/db mice and db/m mice. (D) Expression of selected 10 downregulated mRNAs in db/db mice and db/m mice. *$P < 0.05$ and **$P < 0.01$, versus db/m mice, n = 4. LncRNA, long non-coding RNA; mRNA, massage RNA; qRT-PCR, quantitative real-time polymerase chain reaction.

signaling pathway in diabetic complications, cytokine-cytokine receptor interaction, and chemokine signaling pathway (Fig. 6).

3.5. LncRNA-miRNA-mRNA network analysis

The lncRNA-associated ceRNA mechanism has been demonstrated to participate in the development of diabetic complications. To classify the ceRNA function, 11 DE lncRNAs were selected according to qRT-PCR results. Then, we predicted miRNAs and their target genes in TargetScan and miRanda database, in which the involved genes were limited to the DE mRNAs detected in the microarray, and the predicted miRNA ID was within 1000. GO and KEGG analysis were carried out on DE mRNAs involved in ceRNA function of the candidate lncRNAs. GO analysis presented that the most significantly enriched cellular components was cell part (Fig. 7A). The significantly enriched biological processes were cellular process, immune system process, negative regulation of biological process, cell activation, and cell-cell adhesion (Fig. 7B). For molecular functions, binding, protein binding, fibronectin binding, ion binding, and ion transmembrane transporter activity were enriched (Fig. 7C). The enriched pathways including AGE-RAGE signaling pathway in diabetic complications, influenza A, apoptosis, colorectal cancer, and cell adhesion molecules (CAMs) were associated with ceRNA function of lncRNA (Fig. 7D).

In order to show detailed interactions among lncRNA, miRNA, and mRNA, 3 significantly enriched signaling pathways including AGE-RAGE signaling pathway in diabetic complications, apoptosis, and CAMs in KEGG results were selected to draw lncRNA-miRNA-mRNA networks (Fig. 8A–G). As shown in the networks, each lncRNA has a different number of interacted genes. Among the 4 upregulated lncRNAs, ENSMUST00000160089 had a maximum number of regulated genes in its network, including 23 miRNAs and 18 mRNAs (Fig. 8B), whereas ENSMUST00000099676 was only predicted to target 5 miRNAs and regulate 2 mRNAs (Fig. 8C). The ceRNA function network of ENSMUST00000140392 was the largest one in the 3 downregulated lncRNAs, which was composed of 24 miRNAs and 13 mRNAs (Fig. 8G).

3.6. Correlation analysis between lncRNAs expression and diabetes mellitus pathology

In order to investigate whether lncRNAs alterations were associated with diabetic condition of mice, we further analyzed the correlations between 11 DE lncRNAs expression and blood glucose as well as serum insulin levels. The expression of ENSMUST00000099676, ENSMUST00000123574, ENSMUST00000146010, ENSMUST00000160089, ENSMUST00000175668, ENSMUST00000189055, and ENSMUST00000189909 were positively correlated with blood glucose level (Fig. 9A–G). ENSMUST00000140392, ENSMUST00000140814, and ENSMUST00000150947 levels were negatively correlated with blood glucose level, whereas AK155805 expression was not correlated with it (Fig. 9H–K).

In line with blood glucose, the expression amount of ENSMUST00000099676, ENSMUST00000123574, ENSMUST00000146010, ENSMUST00000160089, ENSMUST00000175668, and ENSMUST00000189909 showed positive correlations with serum insulin level, ENSMUST00000140392 and ENSMUST00000150947 expression showed negative correlations with serum insulin level, while the expression of ENSMUST00000189055, AK155805, and ENSMUST00000140814 showed no

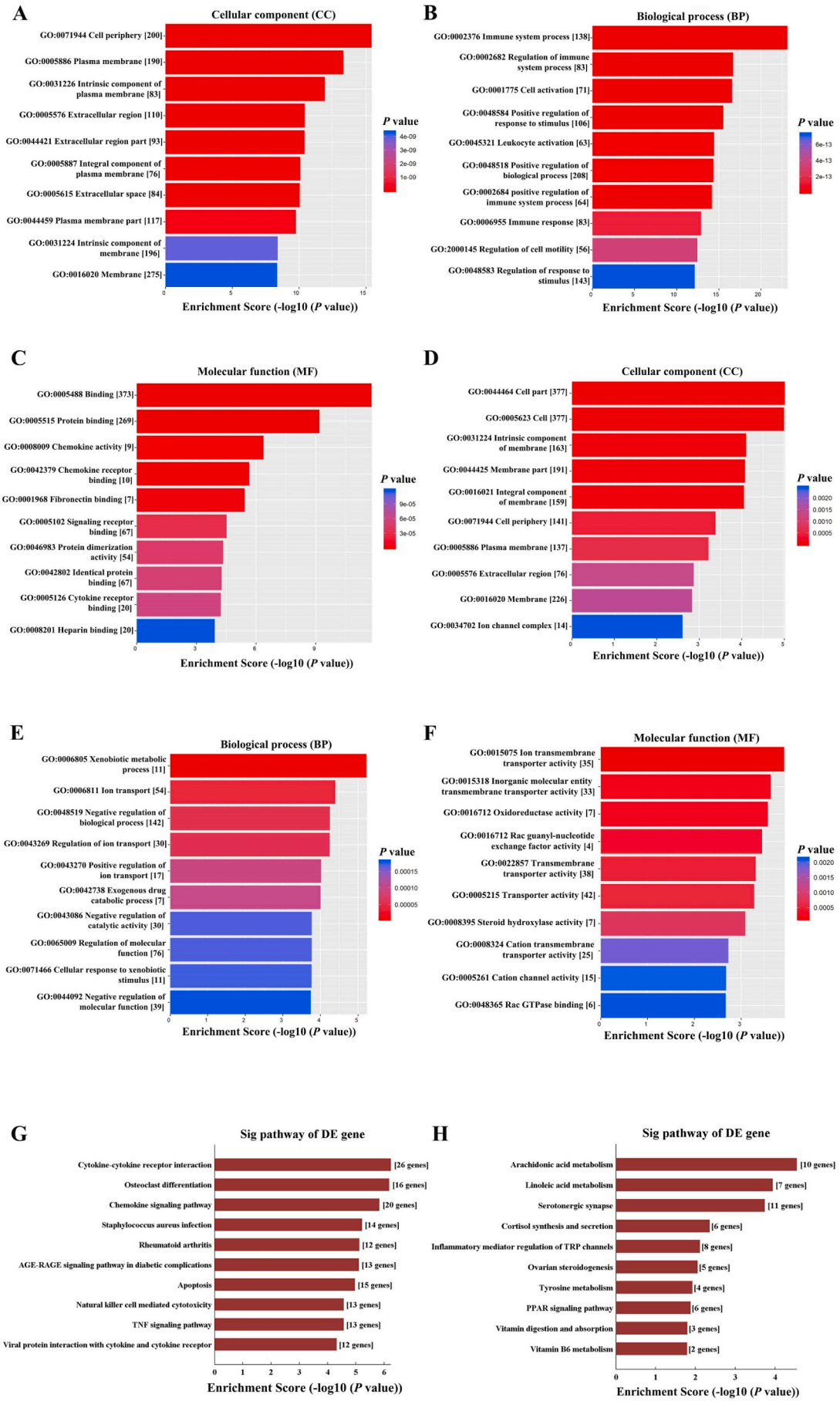

(caption on next page)

Fig. 4. GO and KEGG analysis of differently expressed mRNAs in PGs of db/db mice comparing to db/m mice. (A) GO analysis of upregulated mRNAs on cellular component (CC). (B) GO analysis of upregulated mRNAs on biological process (BP). (C) GO analysis of upregulated mRNAs on molecular function (MF). (D) GO analysis of downregulated mRNAs on CC. (E) GO analysis of downregulated mRNAs on BP. (F) GO analysis of downregulated mRNAs on MF. (G) KEGG pathway analysis of upregulated mRNAs. (H) KEGG pathway analysis of downregulated mRNAs. GO, Gene Ontology; KEGG, Kyoto Encyclopedia of Genes and Genomes; mRNA, massage RNA; PG, parotid gland; DE, differently expressed.

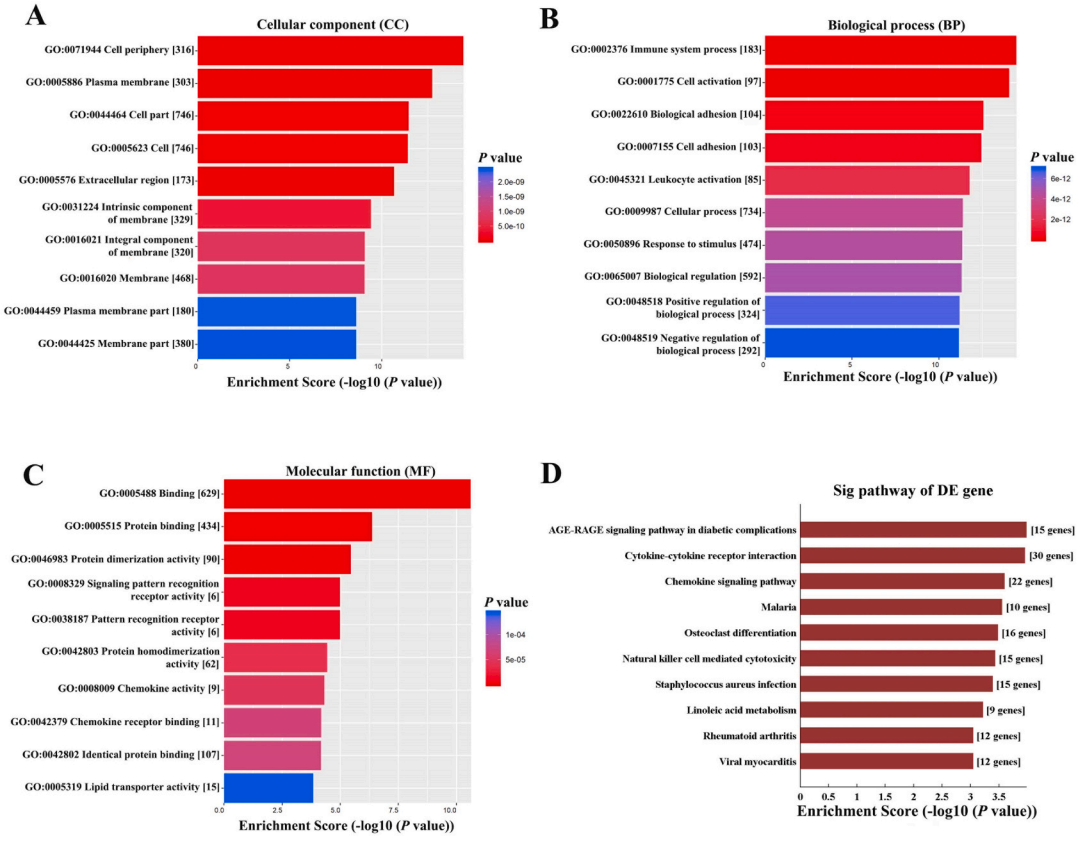

Fig. 5. GO and KEGG analysis based on CNC analysis results of 11 lncRNAs. (A) GO analysis of co-expressed mRNAs on cellular component (CC). (B) GO analysis of co-expressed mRNAs on biological process (BP). (C) GO analysis of co-expressed mRNAs on molecular function (MF). (D) KEGG analysis of co-expressed mRNAs. GO, Gene Ontology; KEGG, Kyoto Encyclopedia of Genes and Genomes; CNC, coding–non-coding gene co-expression; lncRNA, long non-coding RNA; mRNA, massage RNA.

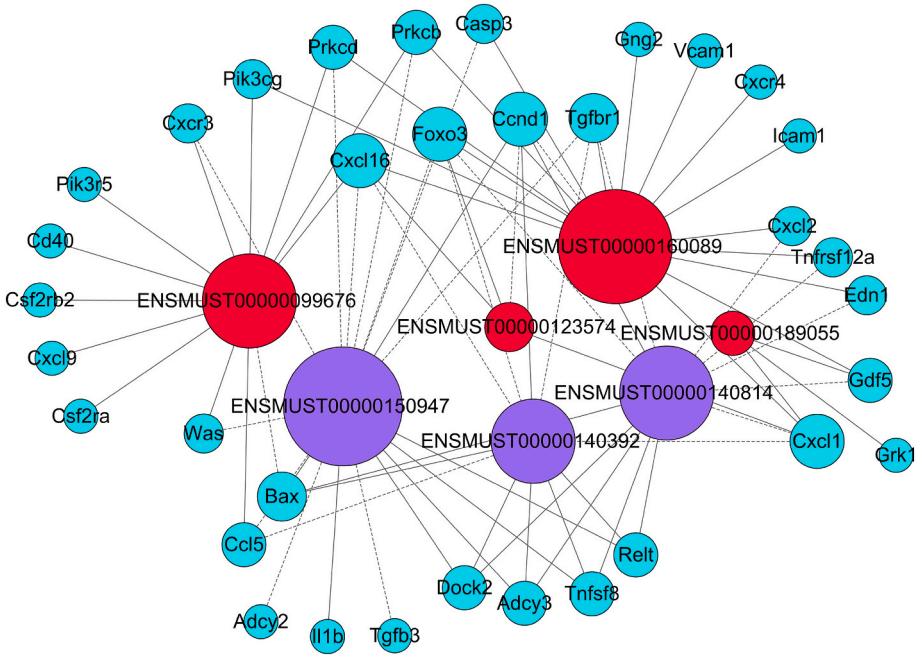

Fig. 6. LncRNA-mRNA co-expression network involving in AGE-RAGE signaling pathway in diabetic complications, cytokine-cytokine receptor interaction, and chemokine signaling pathway. Red nodes represent upregulated lncRNAs; purple nodes represent downregulated lncRNAs; blue nodes represent mRNAs. Positive correlation is a solid line, negative correlation is a dashed line. LncRNA, long non-coding RNA; mRNA, massage RNA; AGE, advanced glycation end products; RAGE, receptor of AGE. (For interpretation of the references to color in this figure legend, the reader is referred to the web version of this article.)

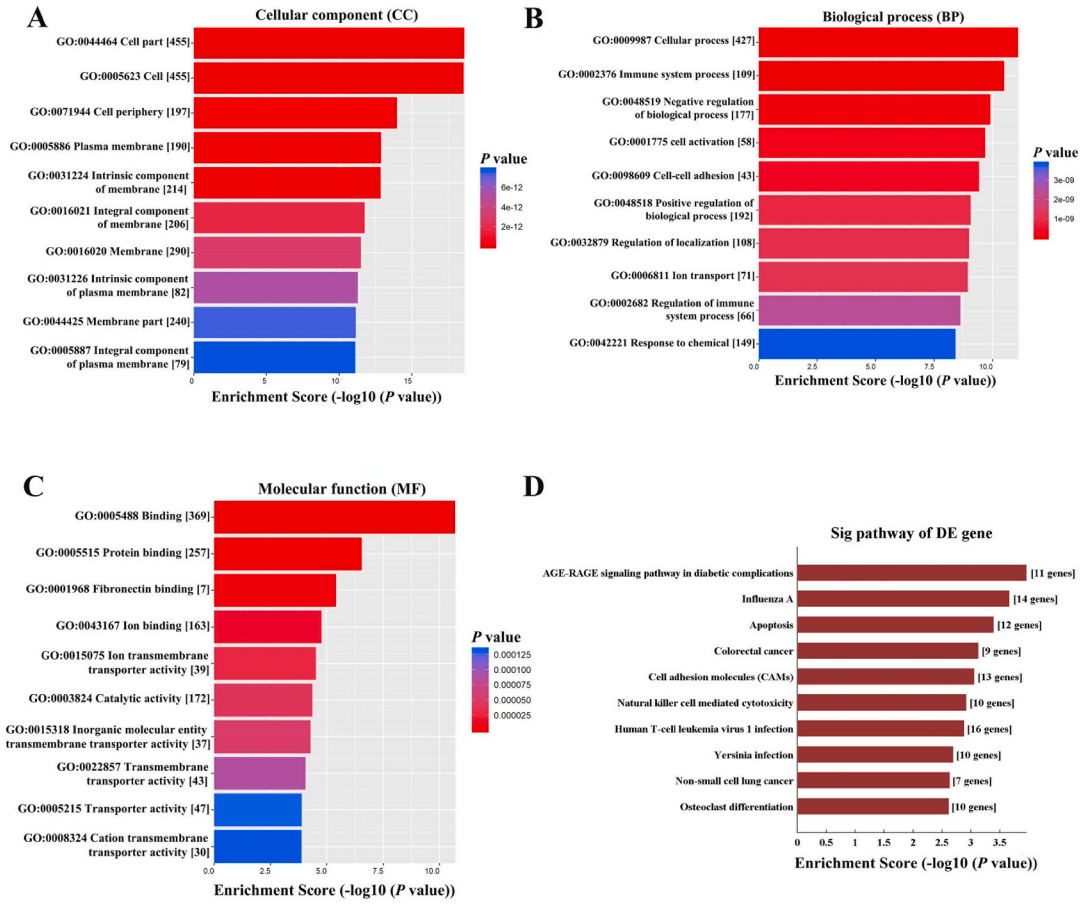

Fig. 7. GO and KEGG analysis based on ceRNA analysis results of 11 lncRNAs. (A) GO analysis of ceRNA function-related mRNAs on cellular component (CC). (B) GO analysis of ceRNA function-related mRNAs on biological process (BP). (C) GO analysis of ceRNA function-related mRNAs on molecular function (MF). (D) KEGG analysis of ceRNA function-related mRNAs. GO, Gene Ontology; KEGG, Kyoto Encyclopedia of Genes and Genomes; ceRNA, competing endogenous RNA; lncRNA, long non-coding RNA; mRNA, massage RNA.

correlation with serum insulin (Fig. 10A–K).

4. Discussion

Our study found that lncRNA and mRNA expression profiles were altered in PG under diabetic condition. Bioinformatic analysis on DE mRNA revealed that activated inflammation process and downregulated ion transport were enriched in diabetic PG. Functional analysis of DE lncRNA suggested that activation of inflammation response through AGE-RAGE signaling pathway, cytokine-cytokine receptor interaction, and chemokine signaling pathway may involve in CNC function of lncRNA in the process of DM-induced PG impairment. In addition, AGE-RAGE signaling pathway, apoptosis, and CAMs might be the downstream pathways of ceRNA function, which might contribute to both activated inflammation response and downregulated ion transport in diabetic PG.

LncRNA is a newly found non-coding RNA with multiple biological functions, which is demonstrated to be aberrantly expressed and play essential roles in the pathophysiological process of diabetic complications, providing new avenues for the diagnosis and treatment of these diseases [21–25]. Although the studies based on lncRNAs have been conducted in many DM-impacted organs, lncRNA profile and related mechanism in DM-impaired salivary gland are still unknown. Owing to the cell type and organ-specific expression patterns of lncRNA, it is of great significance to uncover lncRNA profiles in salivary gland under diabetic condition. Here, we identified 1650 DE lncRNAs including 758 upregulated and 892 downregulated, accompanied by 1073 DE mRNAs (563 upregulated and 510 downregulated) in the PGs of DM mice.

The changes in mRNA expression profiles are associated with biological behaviors and functions of cells. The results of GO and KEGG analysis presented that the upregulated mRNAs in diabetic PGs were mostly enriched in immune response and cytokine-cytokine receptor interaction signaling pathway. Studies have shown that type 2 DM is a chronic inflammatory disease with immune dysfunction and increased inflammatory cytokines [26]. Various inflammatory factors produced by the activation of immune system are not only directly involved in insulin resistance, but also closely related to the occurrence of diabetic complications [27,28]. The role of inflammatory modulators in the salivary gland has been well explored in several diseases of salivary gland. Studies have found that the innate and adaptive immunity, as well as the consequent inflammation are the main mechanisms of pSS pathogenesis [29]. Many inflammatory cytokines and receptors such as interleukins (ILs), chemokines, interferons, and tumor necrosis factors (TNFs) are reported to be elevated in the salivary glands of pSS patients, which recruits leucocytes to the glands and leads to glandular destruction and hyposalivation [30–32]. IgG4-related sialadenitis (IgG4-RS) is a chronic fibro-inflammatory disease characterized by swelling of salivary glands and hyposalivation. Proinflammatory cytokine TNF-α is found to participate in acinar injury in IgG4-RS through inhibiting ERK1/2-mediated autophagic flux [33]. Moreover, inflammatory cytokines are proved to damage secretory functions of salivary gland in diabetic condition. An infiltration of inflammatory cells and increased expression of IL-6 and TNF-α, as well as decreased salivary flow rate are observed in the PG from DM rat [34]. Solinas et al. find that the storage of lipid droplets in diabetic PGs induced by high-fat diet activates the secretion of inflammatory cytokines, including TNF-α, IL-6, and IL-1β, which is

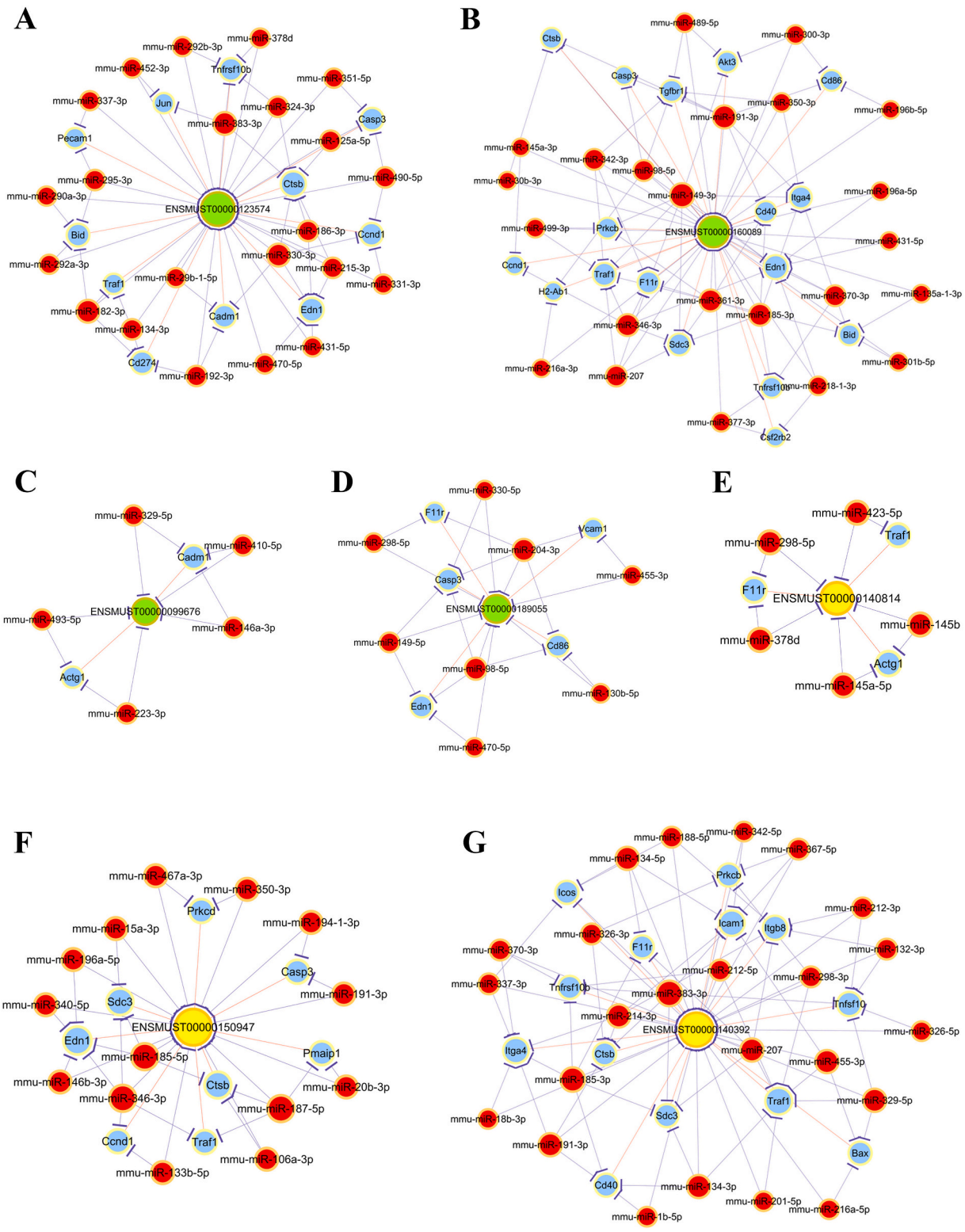

Fig. 8. LncRNA-miRNA-mRNA network involving in AGE-RAGE signaling pathway in diabetic complications, apoptosis, and cell adhesion molecules. (A) LncRNA-miRNA-mRNA network of ENSMUST00000123574. (B) LncRNA-miRNA-mRNA network of ENSMUST00000160089. (C) LncRNA-miRNA-mRNA network of ENSMUST00000099676. (D) LncRNA-miRNA-mRNA network of ENSMUST00000189055. (E) LncRNA-miRNA-mRNA network of ENSMUST00000140814. (F) LncRNA-miRNA-mRNA network of ENSMUST00000150947. (G) LncRNA-miRNA-mRNA network of ENSMUST00000140392. Green nodes represent upregulated lncRNAs; yellow nodes represent downregulated lncRNAs; red nodes represent miRNAs; blue nodes represent mRNAs. Purple lines with T-shape arrow represent directed relationships; orange lines without arrow represent undirected relationships. LncRNA, long non-coding RNA; miRNA, microRNA; mRNA, massage RNA; AGE, advanced glycation end products; RAGE, receptor of AGE. (For interpretation of the references to color in this figure legend, the reader is referred to the web version of this article.)

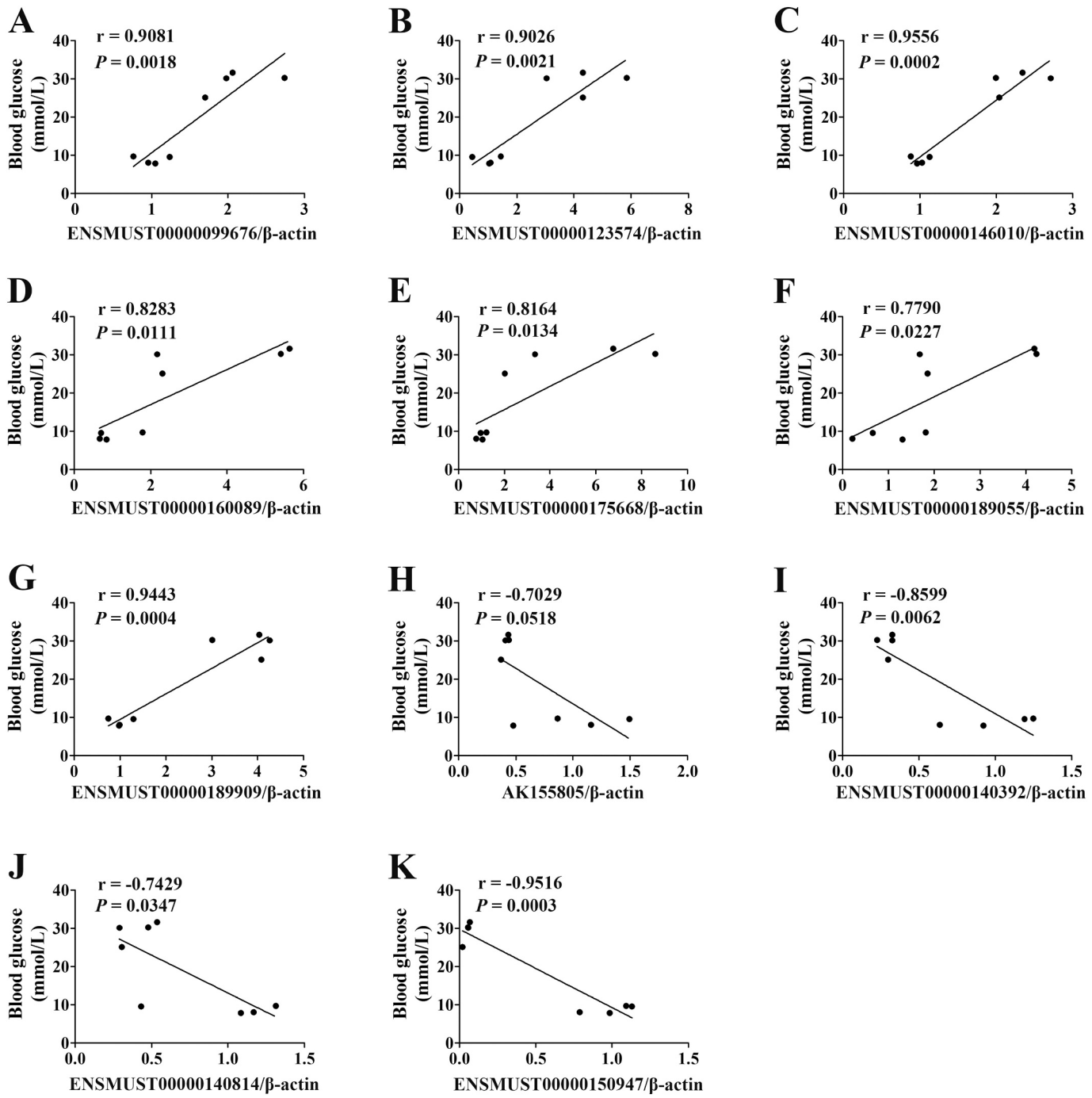

Fig. 9. Correlation analysis between lncRNAs expression and blood glucose level. (A) Correlation between ENSMUST00000099676 and blood glucose level. (B) Correlation between ENSMUST00000123574 and blood glucose level. (C) Correlation between ENSMUST00000146010 and blood glucose level. (D) Correlation between ENSMUST00000160089 and blood glucose level. (E) Correlation between ENSMUST00000175668 and blood glucose level. (F) Correlation between ENSMUST00000189055 and blood glucose level. (G) Correlation between ENSMUST00000189909 and blood glucose level. (H) Correlation between AK155805 and blood glucose level. (I) Correlation between ENSMUST00000140392 and blood glucose level. (J) Correlation between ENSMUST00000140814 and blood glucose level. (K) Correlation between ENSMUST00000150947 and blood glucose level. n = 8. LncRNA, long non-coding RNA.

associated with the dysfunction of diabetic PG [35]. Thus, inflammatory modulators can affect salivation through regulating inflammation response or other biological process like autophagy in salivary gland. Here, the upregulated some mRNAs might activate immune response through promoting inflammatory cytokines synthesis and the interaction with their receptors in the PGs of DM mice, which might contribute to the dysfunction of diabetic PG. On the other hand, GO analysis of downregulated genes was enriched in ion transport process. Ion transport is crucial in the process of saliva secretion, which can regulate water passing across epithelial cells of salivary glands, and a disruption of ion transport especially Ca^{2+} can notably influence salivation [36]. The increased inflammation and reduced intracellular calcium transient rising rate are observed in high-fat diet rat, which causes obese-insulin resistance, leading to pathophysiological alteration of submandibular glands [37]. Therefore, our results predicted that upregulated inflammation response and downregulated ion transport in PG might be crucial in diabetic hyposalivation. However, the specific mechanism needs further study.

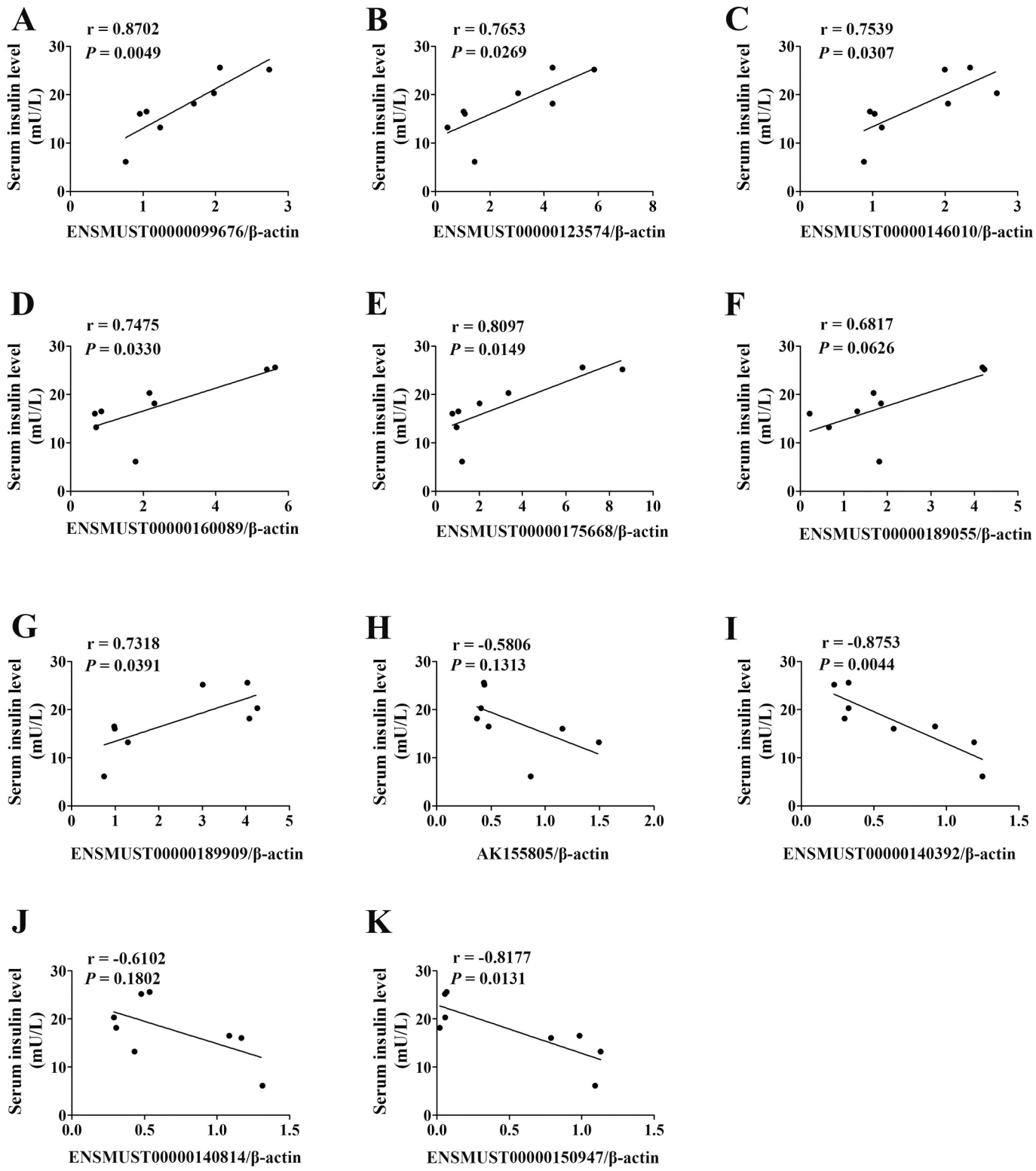

Fig. 10. Correlation analysis between lncRNAs expression and serum insulin level. (A) Correlation between ENSMUST00000099676 and serum insulin level. (B) Correlation between ENSMUST00000123574 and serum insulin level. (C) Correlation between ENSMUST00000146010 and serum insulin level. (D) Correlation between ENSMUST00000160089 and serum insulin level. (E) Correlation between ENSMUST00000175668 and serum insulin level. (F) Correlation between ENSMUST00000189055 and serum insulin level. (G) Correlation between ENSMUST00000189909 and serum insulin level. (H) Correlation between AK155805 and serum insulin level. (I) Correlation between ENSMUST00000140392 and serum insulin level. (J) Correlation between ENSMUST00000140814 and serum insulin level. (K) Correlation between ENSMUST00000150947 and serum insulin level. n = 8. LncRNA, long non-coding RNA.

To identify the roles of the DE lncRNAs in the pathophysiological alterations of diabetic PG, we constructed a lncRNA-mRNA co-expression network on candidate 11 lncRNAs and DE mRNA from microarray. Further bioinformatic analysis indicated that the genes involved in CNC network were mostly enriched in AGE-RAGE signaling pathway in diabetic complication. AGE-RAGE signaling pathway is regarded as a signal to induce inflammation [38,39]. Studies show that AGE treatment can significantly increase IL-6 mRNA expression and secretion through activating NF-κB, a key component in inflammatory cytokine production, thereby enhancing macrophage differentiation into proinflammatory M1 phenotype. However, this effect is reversed by using RAGE antagonist [40]. Other inflammation-associated signaling pathways including cytokine-cytokine receptor interaction and chemokine signaling pathway were also enriched in diabetic PG. Moreover, among the 11 lncRNAs, the upregulated ENSMUST00000099676 (AW112010) is reported to be involved in inflammation response. Activation of T-cells leads to the increase of AW112010, which exerts its proinflammatory property by inhibiting IL-10 expression [41]. The translation of the non-canonical open reading frames within Aw112010 is essential for mucosal immunity, which contributes to intestinal inflammation by promoting the production of inflammatory cytokines IL-12p40 and IL-6, as well as inhibiting the release of anti-inflammatory IL-10 [42]. Collectively, the potential CNC function of DE 11 lncRNA, especially ENSMUST00000099676, was to trigger inflammation response by a network comprising AGE, cytokines, chemokines, and their target receptors, which were closely related to the pathophysiological injury of diabetic PG.

Another typical function of lncRNA is to act as a ceRNA for interacting with specific miRNA, thereby exerting its negative regulation in gene expression. Therefore, we established ceRNA network on the 11 DE lncRNAs. The results showed that the DE mRNAs involved in ceRNA network were enriched in AGE-RAGE signaling pathway in diabetic complication, apoptosis and CAMs. Increasing studies reveal that many diabetes-impaired tissues exhibit a higher degree of apoptosis, which is documented to induce dysfunction of salivary gland under pathological statuses such as pSS, post-irradiation, and high-fat diet [43–47]. Local delivery of keratinocyte growth factor-1 into the irradiated salivary glands could protect radiation-induced cell damages by suppressing p53-mediated apoptosis, thus preventing submandibular glands hypofunction in mice [48]. However, the role of apoptosis in diabetic salivary gland is rarely reported. For CAMs, several CAMs, such as vascular cell adhesion molecule 1, intercellular adhesion molecule 1, and integrin are proved to play crucial roles in modulating inflammatory process [49]. Upon cytokine stimulation, CAMs genes are upregulated in order to facilitate leukocyte adhesion and migration to sites of inflammation [50]. Moreover, CAMs are reported to regulate Ca^{2+} influx in neurons. In response to the stimuli of the CAMs, intracellular Ca^{2+} levels of neural cells are increased by activating several classes of voltage-dependent Ca^{2+} channels [51]. Studies demonstrate that Ca^{2+} is a critical factor in the control of salivary gland function, an increase in intracellular Ca^{2+} concentrations can regulate the ion fluxes required to drive vectorial fluid secretion, thereby promoting saliva secretion [52]. Taken together, AGE-RAGE signaling pathway, apoptosis and CAMs are three critical downstream pathways for the lncRNA ceRNA function in contribution to the dysfunction of diabetic PG through modulating inflammation, apoptosis, and ion transport processes.

The important pathogenic characteristics of DM are abnormal insulin and glucose metabolism, which are demonstrated to influence salivary gland function by regulating mRNA or protein expression. Early studies have showed that insulin had a rapid, direct effect on the rate of protein synthesis such as secretory enzyme, peroxidase in the rat submandibular gland [53,54]. Insulin can induce the phosphorylation of its receptor and activate elements involved in the early steps of insulin signaling including Shc, JAK-2, and STAT-1 in salivary gland [55]. Hyperglycemia increases the deposition of extracellular matrix proteins in the rat PG through increasing of transforming growth factor-β2 expression and signal [56]. Our previous study reveals that high glucose downregulates aquaporin 5 mRNA and protein expression, contributing to hyposecretion of diabetic submandibular gland [57]. Moreover, therapies targeting insulin action or eliminating hyperglycemia are proved to be effective in improving secretory function of salivary gland [58–60]. Therefore, the abnormalities of protein or mRNA expression in salivary gland might closely related to DM pathology. In order to classify the relationship between DM pathology and changes in PG lncRNAs expression, we further analyzed the correlations between 11 candidate lncRNAs and blood glucose as well as serum insulin levels. The results showed that all upregulated lncRNAs were positively correlated with blood glucose level, the downregulated lncRNAs excepting AK155805 were negatively correlated with blood glucose. For serum insulin level, 3 lncRNAs including 1 upregulated and 2 downregulated showed no statistical correlation. These data suggested that most of the altered lncRNAs in diabetic PG might involve in DM pathological progress.

5. Conclusion

This study identified aberrant expression profiles of lncRNAs and mRNAs in the PGs of DM mice, which were correlated with the changes of higher blood glucose and serum insulin levels. The potential role of significantly DE lncRNAs might be the regulation of inflammation, apoptosis, and ion transport biological processes through AGE-RAGE, cytokine-cytokine receptor interaction, chemokine, apoptosis, and CAMs signaling pathways, which contributed to the dysfunction of diabetic PG. These findings expand our understanding of lncRNA in diabetic PG. By establishing regulatory networks, our study helps to reveal the potential mechanisms of lncRNA in the pathogenesis of DM-related hyposalivation, which provides valuable resources for further investigation.

CRediT authorship contribution statement

Yan Huang contributed to the data curation, investigation, visualization, and original draft. Hui-Min Liu contributed to the methodology, software, and validation. Li-Ling Wu contributed to conceptualization, formal analysis, supervision, and review & editing. Guang-Yan Yu, Ruo-Lan Xiang contributed to the funding acquisition, project administration, resources, and review & editing.

Declaration of competing interest

The authors declare that there are no conflicts of interest.

Acknowledgments

This work was supported by the National Natural Science Foundation of China (grant number 81974151, 2020) and the Beijing Natural Science Foundation (grant number 7202078, 2019).

References

[1] A. Poznyak, A.V. Grechko, P. Poggio, V.A. Myasoedova, V. Alfieri, A.N. Orekhov, The diabetes mellitus-atherosclerosis connection: the role of lipid and glucose metabolism and chronic inflammation, Int. J. Mol. Sci. 21 (5) (2020) 1835.
[2] K.R. Bhattarai, R. Junjappa, M. Handigund, H.R. Kim, H.J. Chae, The imprint of salivary secretion in autoimmune disorders and related pathological conditions, Autoimmun. Rev. 17 (4) (2018) 376–390.
[3] M.A. Nazir, L. AlGhamdi, M. AlKadi, N. AlBeajan, L. AlRashoudi, M. AlHussan, The burden of diabetes, its oral complications and their prevention and management, Open Access Maced J Med Sci 6 (8) (2018) 1545–1553.
[4] A.M.L. Pedersen, C.E. Sørensen, G.B. Proctor, G.H. Carpenter, J. Ekström, Salivary secretion in health and disease, J. Oral Rehabil. 45 (9) (2018) 730–746.
[5] M.R. Quirino, E.G. Birman, C.R. Paula, Oral manifestations of diabetes mellitus in controlled and uncontrolled patients, Braz. Dent. J. 6 (2) (1995) 131–136.
[6] S.B. Russotto, Asymptomatic parotid gland enlargement in diabetes mellitus, Oral Surg Oral Med Oral Pathol 52 (6) (1981) 594–598.

[7] L. Arnes, I. Akerman, D.A. Balderes, J. Ferrer, L. Sussel, βlinc1 encodes a long noncoding RNA that regulates islet β-cell formation and function, Genes Dev. 30 (5) (2016) 502–507.
[8] C. Carda, M. Carranza, A. Arriaga, A. Díaz, A. Peydró, M.E. Gomez de Ferraris, Structural differences between alcoholic and diabetic parotid sialosis, Med. Oral Patol. Oral Cir. Bucal. 10 (4) (2005) 309–314.
[9] C. Carda, N. Mosquera-Lloreda, L. Salom, M.E. Gomez de Ferraris, A. Peydró, Structural and functional salivary disorders in type 2 diabetic patients, Med. Oral Patol. Oral Cir. Bucal. 11 (4) (2006) E309–E314.
[10] M.A. Lilliu, F. Loy, M. Cossu, P. Solinas, R. Isola, M. Isola, Morphometric study of diabetes related alterations in human parotid gland and comparison with submandibular gland, Anat Rec (Hoboken) 298 (11) (2015) 1911–1918.
[11] Y. Huang, Q.Y. Mao, X.J. Shi, X. Cong, Y. Zhang, L.L. Wu, G.Y. Yu, R.L. Xiang, Disruption of tight junctions contributes to hyposalivation of salivary glands in a mouse model of type 2 diabetes, J. Anat. 237 (3) (2020) 556–567.
[12] I.M. Dykes, C. Emanueli, Transcriptional and post-transcriptional gene regulation by long non-coding RNA, Genomics Proteomics Bioinformatics 15 (3) (2017) 177–186.
[13] U.H. Weidle, F. Birzele, G. Kollmorgen, R. Rüger, Long non-coding RNAs and their role in metastasis, Cancer Genomics Proteomics 14 (3) (2017) 143–160.
[14] P. Sandhya, K. Joshi, V. Scaria, Long noncoding RNAs could be potential key players in the pathophysiology of Sjögren's syndrome, Int. J. Rheum. Dis. 18 (8) (2015) 898–905.
[15] H. Shi, N. Cao, Y. Pu, L. Xie, L. Zheng, C. Yu, Long non-coding RNA expression profile in minor salivary gland of primary Sjögren's syndrome, Arthritis Res Ther 18 (1) (2016), 109.
[16] J. Fu, H. Shi, B. Wang, T. Zhan, Y. Shao, L. Ye, S. Wu, C. Yu, L. Zheng, LncRNA PVT1 links Myc to glycolytic metabolism upon CD4(+) T cell activation and Sjögren's syndrome-like autoimmune response, J. Autoimmun. 107 (2019), 102358.
[17] W. Xu, L. Liu, H. Lu, J. Fu, C. Zhang, W. Yang, S. Shen, Dysregulated long noncoding RNAs in pleomorphic adenoma tissues of pleomorphic adenoma gene 1 transgenic mice, Mol. Med. Rep. 19 (6) (2019) 4735–4742.
[18] S.D. Feng, J.H. Yang, C.H. Yao, S.S. Yang, Z.M. Zhu, D. Wu, H.Y. Ling, L. Zhang, Potential regulatory mechanisms of lncRNA in diabetes and its complications, Biochem. Cell Biol. 95 (3) (2017) 361–367.
[19] A. Leung, R. Natarajan, Long noncoding RNAs in diabetes and diabetic complications, Antioxid. Redox Signal. 29 (11) (2018) 1064–1073.
[20] D. Zheng, Y. Zhang, Y. Hu, J. Guan, L. Xu, W. Xiao, Q. Zhong, C. Ren, J. Lu, J. Liang, J. Hou, Long noncoding RNA Crnde attenuates cardiac fibrosis via Smad3-Crnde negative feedback in diabetic cardiomyopathy, FEBS J. 286 (9) (2019) 1645–1655.
[21] W. Zhang, J. Zheng, X. Hu, L. Chen, Dysregulated expression of long noncoding RNAs serves as diagnostic biomarkers of type 2 diabetes mellitus, Endocrine 65 (3) (2019) 494–503.
[22] M. Wu, Y. Feng, X. Shi, Advances with long non-coding RNAs in diabetic peripheral neuropathy, Diabetes Metab Syndr Obes 13 (2020) 1429–1434.
[23] L. Xia, M. Song, Role of non-coding RNA in diabetic cardiomyopathy, Adv. Exp. Med. Biol. 1229 (2020) 181–195.
[24] L.Y. Ci, D.S. Liu, J.Q. Yang, Y.Z. Liu, C.L. Li, X. Zhang, C.M. Ma, R.T. Hu, Expression of long non-coding RNA and mRNA in the hippocampus of mice with type 2 diabetes, Mol. Med. Rep. 18 (6) (2018) 4960–4968.
[25] X. Ge, B. Xu, W. Xu, L. Xia, Z. Xu, L. Shen, W. Peng, S. Huang, Long noncoding RNA GAS5 inhibits cell proliferation and fibrosis in diabetic nephropathy by sponging miR-221 and modulating SIRT1 expression, Aging (Albany NY) 11 (20) (2019) 8745–8759.
[26] M. Kanbay, E.M. Onal, B. Afsar, T. Dagel, A. Yerlikaya, A. Covic, N.D. Vaziri, The crosstalk of gut microbiota and chronic kidney disease: role of inflammation, proteinuria, hypertension, and diabetes mellitus, Int. Urol. Nephrol. 50 (8) (2018) 1453–1466.
[27] A.B. Goldfine, S.E. Shoelson, Therapeutic approaches targeting inflammation for diabetes and associated cardiovascular risk, J. Clin. Invest. 127 (1) (2017) 83–93.
[28] M.Y. Sun, S.J. Wang, X.Q. Li, Y.L. Shen, J.R. Lu, X.H. Tian, K. Rahman, L.J. Zhang, H. Nian, H. Zhang, CXCL6 promotes renal interstitial fibrosis in diabetic nephropathy by activating JAK/STAT3 signaling pathway, Front. Pharmacol. 10 (2019) 224.
[29] C. Rizzo, G. Grasso, G.M. Destro Castaniti, F. Ciccia, G. Guggino, Primary Sjögren syndrome: focus on innate immune cells and inflammation, Vaccines (Basel) 8 (2) (2020) 272.
[30] S.L.M. Blokland, M.R. Hillen, A.A. Kruize, S. Meller, B. Homey, G.M. Smithson, T. Radstake, J.A.G. van Roon, Increased CCL25 and T helper cells expressing CCR9 in the salivary glands of patients with primary Sjögren's syndrome: potential new axis in lymphoid neogenesis, Arthritis Rheumatol 69 (10) (2017) 2038–2051.
[31] X. Chen, L.A. Aqrawi, T.P. Utheim, B. Tashbayev, A. Utheim Ø, S. Reppe, L. H. Hove, B.B. Herlofson, P.B. Singh, Ø. Palm, H.K. Galtung, J.C.L. Jensen, Elevated cytokine levels in tears and saliva of patients with primary Sjögren's syndrome correlate with clinical ocular and oral manifestations, Sci. Rep. 9 (1) (2019) 7319.
[32] Z. Liu, F. Li, A. Pan, H. Xue, S. Jiang, C. Zhu, M. Jin, J. Fang, X. Zhu, M.A. Brown, X. Wang, Elevated CCL19/CCR7 expression during the disease process of primary Sjögren's syndrome, Front. Immunol. 10 (2019) 795.
[33] X. Hong, S.N. Min, Y.Y. Zhang, Y.T. Lin, F. Wang, Y. Huang, G.Y. Yu, L.L. Wu, H. Y. Yang, TNF-α suppresses autophagic flux in acinar cells in IgG4-related sialadenitis, J. Dent. Res. 98 (12) (2019) 1386–1396.
[34] S.Y. Chen, Y. Wang, C.L. Zhang, Z.M. Yang, Decreased basal and stimulated salivary parameters by histopathological lesions and secretory dysfunction of parotid and submandibular glands in rats with type 2 diabetes, Exp Ther Med 19 (4) (2020) 2707–2719.
[35] G. Solinas, M. Karin, JNK1 and IKKbeta: molecular links between obesity and metabolic dysfunction, FASEB J. 24 (8) (2010) 2596–2611.
[36] I. Ambudkar, Calcium signaling defects underlying salivary gland dysfunction, Biochim Biophys Acta Mol Cell Res 1865 (11 Pt B) (2018) 1771–1777.
[37] J. Ittichaicharoen, N. Apaijai, P. Tanajak, P. Sa-Nguanmoo, N. Chattipakorn, S. C. Chattipakorn, Impaired mitochondria and intracellular calcium transients in the salivary glands of obese rats, Appl Physiol Nutr Metab 42 (4) (2017) 420–429.
[38] J.H. Meertens, H.L. Nienhuis, J.D. Lefrandt, C.G. Schalkwijk, K. Nyyssönen, J. J. Ligtenberg, A.J. Smit, J.G. Zijlstra, D.J. Mulder, The course of skin and serum biomarkers of advanced glycation endproducts and its association with oxidative stress, inflammation, disease severity, and mortality during ICU admission in critically ill patients: results from a prospective pilot study, PLoS One 11 (8) (2016), e0160893.
[39] P. Younessi, A. Yoonessi, Advanced glycation end-products and their receptor-mediated roles: inflammation and oxidative stress, Iran J Med Sci 36 (3) (2011) 154–166.
[40] A. Ohtsu, Y. Shibutani, K. Seno, H. Iwata, T. Kuwayama, K. Shirasuna, Advanced glycation end products and lipopolysaccharides stimulate interleukin-6 secretion via the RAGE/TLR4-NF-κB-ROS pathways and resveratrol attenuates these inflammatory responses in mouse macrophages, Exp Ther Med 14 (5) (2017) 4363–4370.
[41] X. Yang, M. Bam, W. Becker, P.S. Nagarkatti, M. Nagarkatti, Long noncoding RNA AW112010 promotes the differentiation of inflammatory T cells by suppressing IL-10 expression through histone demethylation, J. Immunol. 205 (4) (2020) 987–993.
[42] R. Jackson, L. Kroehling, A. Khitun, W. Bailis, A. Jarret, A.G. York, O.M. Khan, J. R. Brewer, M.H. Skadow, C. Duizer, C.C.D. Harman, L. Chang, P. Bielecki, A. G. Solis, H.R. Steach, S. Slavoff, R.A. Flavell, The translation of non-canonical open reading frames controls mucosal immunity, Nature 564 (7736) (2018) 434–438.
[43] T. Tomita, Apoptosis in pancreatic β-islet cells in type 2 diabetes, Bosn J Basic Med Sci 16 (3) (2016) 162–179.
[44] X. Dong, S. Yu, Y. Wang, M. Yang, J. Xiong, N. Hei, B. Dong, Q. Su, J. Chen, (Pro) renin receptor-mediated myocardial injury, apoptosis, and inflammatory response in rats with diabetic cardiomyopathy, J. Biol. Chem. 294 (20) (2019) 8218–8226.
[45] R.S. Wang, T.T. Zhang, Z.H. Xu, K. Hu, Y. Shi, S. Long, H.Y. Yue, Injury in minipig parotid glands following fractionated exposure to 30 Gy of lonizing radiation, Otolaryngol Head Neck Surg 151 (1) (2014) 100–106.
[46] P. Li, Y. Yang, Y. Jin, R. Zhao, C. Dong, W. Zheng, T. Zhang, J. Li, Z. Gu, B7-H3 participates in human salivary gland epithelial cells apoptosis through NF-κB pathway in primary Sjögren's syndrome, J. Transl. Med. 17 (1) (2019), 268.
[47] A. Zalewska, M. Maciejczyk, J. Szulimowska, M. Imierska, A. Błachnio-Zabielska, High-fat diet affects ceramide content, disturbs mitochondrial redox balance, and induces apoptosis in the submandibular glands of mice, Biomolecules 9 (12) (2019) 877.
[48] J.S. Choi, H.S. Shin, H.Y. An, Y.M. Kim, J.Y. Lim, Radioprotective effects of Keratinocyte Growth Factor-1 against irradiation-induced salivary gland hypofunction, Oncotarget 8 (8) (2017) 13496–13508.
[49] O.J. Mezu-Ndubuisi, A. Maheshwari, The role of integrins in inflammation and angiogenesis, Pediatr. Res. (2020), https://doi.org/10.1038/s41390-020-01177-9.
[50] V. Burgos, C. Paz, K. Saavedra, N. Saavedra, M.A. Foglio, L.A. Salazar, Drimenol, isodrimeninol and polygodial isolated from Drimys winteri reduce monocyte adhesion to stimulated human endothelial cells, Food Chem. Toxicol. 146 (2020), 111775.
[51] L. Sheng, I. Leshchyns'ka, V. Sytnyk, Cell adhesion and intracellular calcium signaling in neurons, Cell Commun Signal 11 (2013) 94.
[52] I.S. Ambudkar, Ca^{2+} signaling and regulation of fluid secretion in salivary gland acinar cells, Cell Calcium 55 (6) (2014) 297–305.
[53] L.C. Anderson, B.L. Shapiro, The effect of alloxan diabetes and insulin on the rate of protein synthesis in the rat submandibular gland, Horm. Metab. Res. 12 (2) (1980) 47–50.
[54] L.C. Anderson, Insulin-stimulated protein synthesis in submandibular acinar cells: interactions with adrenergic and cholinergic agonists, Horm. Metab. Res. 20 (1) (1988) 20–23.
[55] E.M. Rocha, A.E. Hirata, E.M. Carneiro, M.J. Saad, L.A. Velloso, Impact of gender on insulin signaling pathway in lacrimal and salivary glands of rats, Endocrine 18 (2) (2002) 191–199.
[56] M.L. Lamers, F.A. Gimenes, F.N. Nogueira, J. Nicolau, P. Gama, M.F. Santos, Chronic hyperglycaemia increases TGFbeta2 signaling and the expression of extracellular matrix proteins in the rat parotid gland, Matrix Biol. 26 (7) (2007) 572–582.
[57] Y. Huang, X. Shi, Q. Mao, Y. Zhang, X. Cong, X. Zhang, Z. Zhang, L. Wu, R. Xiang, G. Yu, Aquaporin 5 is degraded by autophagy in diabetic submandibular gland, Sci. China Life Sci. 61 (9) (2018) 1049–1059.
[58] A.M. Rowzee, P.J. Perez-Riveros, C. Zheng, S. Krygowski, B.J. Baum, N.X. Cawley, Expression and secretion of human proinsulin-B10 from mouse salivary glands: implications for the treatment of type I diabetes mellitus, PLoS One 8 (3) (2013), e59222.
[59] C.Y. Fukuoka, G. Torres Schröter, J. Nicolau, A. Simões, Low-power laser irradiation in salivary glands reduces glycemia in streptozotocin-induced diabetic female rats, J. Biophotonics 9 (11–12) (2016) 1246–1254.
[60] C.Y. Fukuoka, A. Simões, T. Uchiyama, V.E. Arana-Chavez, Y. Abiko, N. Kuboyama, U.K. Bhawal, The effects of low-power laser irradiation on inflammation and apoptosis in submandibular glands of diabetes-induced rats, PLoS One 12 (1) (2017), e0169443.